Scilight

Regional Ecology and Management
https://www.sciltp.com/journals/rem

Article

Driving Forces for Synergistic Reduction of Carbon Dioxide Emissions and Ozone Pollution in Chinese Cities

Xiaoyun Hou [1,2], Shiliang Liu [2,*], Shuang Zhao [2,3], Jingting Li [4], Siyang Zhou [2] and Tianyi Yao [5]

[1] School of Civil Engineering and Architecture, Zhejiang Sci-Tech University, Hangzhou 310016, China
[2] State Key Laboratory of Regional Environment and Sustainability, School of Environment, Beijing Normal University, Beijing 100875, China
[3] Key Laboratory of Coastal Environment and Resources of Zhejiang Province, School of Engineering, Westlake University, Hangzhou 310024, China
[4] School of Architecture Planning and Landscape Architecture, Auburn University, Auburn, AL 36849, USA
[5] Marshall School of Business, University of Southern California, Los Angeles, CA 90089, USA
* Correspondence: shiliangliu@bnu.edu.cn

How To Cite: Hou, X.; Liu, S.; Zhao, S.; et al. Driving Forces for Synergistic Reduction of Carbon Dioxide Emissions and Ozone Pollution in Chinese Cities. *Regional Ecology and Management* **2026**, *1*(1), 2

Received: 4 December 2025
Revised: 12 January 2026
Accepted: 15 January 2026
Published: 22 January 2026

Abstract: China's atmosphere is experiencing severe ozone (O_3) pollution and carbon dioxide (CO_2) emissions, posing persistent threats to public health and sustainable development. Previous research has confirmed a synergistic coupling between O_3 pollution and CO_2 emissions, driven by mutual feedback mechanisms associated with climate warming. To gain a deeper understanding of the contribution of socioeconomic activities, we conducted a multi-parameter analysis of driving forces. In this study, we employed a Structural Equation Model (SEM) to quantify the synergistic control mechanisms for urban O_3 pollution and CO_2 emissions. The findings revealed that compared to 2014, urban atmospheric O_3 concentrations in China significantly increased by 2022, and CO_2 emissions mirrored this upward trend. Assessment of health effects showed that the number of all-cause deaths related to O_3 pollution was approximately 198×10^3 in 2022. The SEM results indicated that the tertiary industry GDP and secondary industry GDP contribute most substantially to atmospheric O_3 pollution and CO_2 emissions. This underscored the importance of optimizing industrial structure to reduce environmental impacts. Building upon the exploration of current abatement technologies, we proposed seven recommendations for synergistic control. Our research provides a scientific foundation for the implementation of "Synergistic Pollution Reduction and Carbon Mitigation" in China.

Keywords: socioeconomic factor; carbon dioxide emission; ozone pollution; driving force; national scale

1. Introduction

The World Meteorological Organization's State of the Global Climate 2024 report documents a critical atmospheric threshold, with carbon dioxide (CO_2) concentrations surging to an unprecedented 420 ppm. This level represents a 151% increase over pre-industrial, driving the 2024 global mean temperature to 1.55 °C above 1850–1900 baselines. The main reason for the massive emissions of CO_2 is that modern anthropogenic activities have reintroduced geologically sequestered carbon (originally fixed through photosynthesis over thousands of years) into the atmosphere by coal and oil consumption [1]. China emerges as a main contributor to the CO_2 emissions with rapid urban and economic development [2]. In general, this thermal anomaly poses serious threats to the stability and health of the global ecosystem.

While China has achieved notable reductions in $PM_{2.5}$ concentrations following the implementation of the 2013 Clean Air Act, concurrent increases in tropospheric ozone (O_3) levels reveal critical limitations in current pollution mitigation strategies [3]. In recent years, photochemical smog dominated by O_3 has posed a critical environmental threat to public health [4]. Substantial evidence links O_3 exposure to adverse effects on human cardiovascular and respiratory systems [5], vegetation productivity [6–8] and soil microbial communities [9]. The escalating severity of O_3 pollution underscores the urgent need for targeted, science-driven interventions to address this multifaceted environmental challenge [10,11].

Emerging evidence reveals a synergistic coupling between O_3 pollution and CO_2 emissions, driven by mutual feedback mechanisms in warming climates [12]. On the one hand, global warming and extreme climatic events significantly enhance O_3 formation. An analysis of eastern China's summertime O_3 episodes demonstrates that heatwaves exceeding 10-day duration significantly exacerbate O_3 pollution [13]. Drought-stressed vegetation exhibits significantly reduced O_3 uptake, driving 10–20 ppbv increases in daily maximum 8-h average O_3 concentrations [14]. Notably, the temporal scope of O_3 pollution has expanded beyond summer months, with the baseline temperature rising by 0.03 °C annually [15]. On the other hand, O_3 enters plant leaves via stomatal uptake, triggering excessive reactive oxygen species, which accumulates disrupt chloroplast ultrastructure and impair photosynthetic electron transport [16]. Concurrently, O_3-induced stomatal closure reduces stomatal conductance, thereby suppressing CO_2 assimilation efficiency [17]. Implementation of synergistic mitigation strategies can concurrently reduce O_3 pollution and attenuate radiative forcing contributions to global warming [18].

As a secondary pollutant, ground-level O_3 forms through photochemical reactions between nitrogen oxides (NO_X) and volatile organic compounds (VOCs) under ultraviolet radiation [19,20]. Rapid urbanization and industrialization in China have driven sustained increases in anthropogenic emissions of VOCs and NO_X, a trend compounded by urban heat island effects that further enhance the conversion of precursors [21–23]. Empirical analyses of regulatory monitoring data reveal that most Chinese cities currently exhibit a VOC-limited O_3 formation regime, suggesting VOC reduction should be prioritized in control policies [24]. Nevertheless, continuous reduction of NO_X emission remains critical in O_3 pollution mitigation strategies.

Among various anthropogenic emission sources, industrial production, paint and solvent applications, and mobile sources have been identified as major contributors to urban VOC emissions [25,26]. Also, the influence of biogenic VOC emissions cannot be overlooked [25,27]. Regarding NO_X emissions, fossil fuel combustion, particularly from power generation and vehicles, constitutes the predominant origin [28]. The emission sources of CO_2 are similar to those of O_3 precursors. Global carbon emissions demonstrate strong sectoral concentration, with the electric power sector accounting for approximately 40% of total emissions through both direct production (e.g., power and heat generation) and indirect consumption pathways [29]. The residential sector contributes significantly through indirect consumption pathways, generating nearly 10% of global CO_2 emissions via electricity consumption for lighting and appliances [2,30]. Notably, the transportation sector contributes 24% to direct energy-related emissions through petroleum fuel combustion [31,32]. In China's industrial sector, manufacturing industry present particularly notable carbon emissions. Cement production emits 0.83–0.91 tons of CO_2 per ton of clinker through calcination and fuel combustion processes [33]. Steel manufacturing demonstrates substantially higher carbon intensity at 2.33 tons CO_2 per ton steel, with over 90% of lifecycle emissions occurring during production phases [34]. These findings emphasize the critical need for developing cross-sectoral emission mitigation strategies. To inform such policy development, systematic quantification of sector-specific contributions to both O_3 pollution and CO_2 emissions becomes imperative.

In this study, we compiled comprehensive data on air pollutant concentrations, CO_2 emissions, and various socioeconomic drivers across 290 prefecture-level administrative regions in China for 2022, representing 87% of the nation's total. Additionally, we obtained comparable air pollutant concentrations and CO_2 emissions data for 162 regions in 2014. This research pursued three primary objectives: (1) to analyze decadal trends (2014–2022) in $PM_{2.5}$ and O_3 pollution, identifying current dominant air pollutants in China; (2) to evaluate associated health impacts and economic burdens from air pollution; and (3) to quantify the relative contributions of specific socioeconomic factors driving air pollution and CO_2 emissions. Our findings establish a theoretical foundation for formulating integrated policies addressing both atmospheric pollution mitigation and climate change adaptation strategies.

2. Material and Methods

2.1. Air Pollution and Carbon Dioxide Emissions Data

To continuously monitor urban air pollutant characteristics, China established the National Air Monitoring Network. This network comprises 1537 monitoring sites across 339 cities. Since 2014, it has been tasked primarily with monitoring air pollution and providing hourly data feedback. We derived 24-h average $PM_{2.5}$ concentrations

and average daily maximum 8-h O_3 concentrations for China's prefecture-level cities in 2014 and 2022 from this network. In accordance with China Ambient Air Quality Standards (GB 3095-2012, https://www.mee.gov.cn/ywgz/fgbz/bz/bzwb/dqhjbh/dqhjzlbz/201203/W020250407403788086276.pdf, accessed on 1 June 2025), $PM_{2.5}$ pollution levels were measured at all sites using the β-ray method and micro-oscillation balance method, while O_3 pollution levels were measured using ultraviolet fluorescence method and differential absorption spectroscopy method. Emissions Database for Global Atmospheric Research is an open-source database providing greenhouse gas emission data for all countries/regions on a 0.1° × 0.1° grid. Using this inventory, we also extracted total CO_2 emission data on urban scale in 2014 and 2022.

2.2. Health and Socioeconomic Data

Baseline data on residents' all-cause mortality were sourced from the China City Statistical Yearbook (www.stats.gov.cn) and the National Population Health Science Data Center (https://www.ncmi.cn/). We also selected four explanatory variables from the City Statistical Yearbook and China's National Bureau of Statistics (www.stats.gov.cn) to assess economic burden, including the consumer price index (CPI), per capita Gross Domestic Product (GDP), purchasing power parity (PPP, adjusted by GDP per capita), and permanent resident population size.

According to relevant literature, we selected 14 socioeconomic driving forces contributing to pollution in 2022, which were categorized as follows: industrial scale, city size, and residents' activities (Table 1). Statistical analysis revealed significant associations ($p < 0.05$) between these socioeconomic indicators and pollution/emission data.

Table 1. Selected driving forces and their corresponding references.

Driving Forces	Reference Sources
Industrial scale	
Primary industry GDP	[35,36]
Secondary industry GDP	[25,33,34,37–39]
Tertiary industry GDP	[40]
Power generation	[27,29,31]
Natural gas consumption	[29]
Electricity consumption for industry	[29,39]
City size	
Urban built-up area	[27,30,33,34]
Resident population	[2,27,41]
Residents' activities	
Total retail sales of consumer goods	[38]
Volume of road haulage	[31,38]
Household electricity consumption	[2,29]
Civilian vehicles	[25,26,28,32,37,41,42]
Heating area	[31]
Green area	[25,27,37]

2.3. Statistical Analysis

Using air pollution and CO_2 emissions data, we first analyzed trends in air pollutants across urban China from 2014 to 2022. Next, we calculated the health impacts associated with the air pollutants. Finally, we employed structural equation model (SEM) to examine how socioeconomic factors affect air pollution and CO_2 emissions. The schematic diagram of the study framework was shown in Figure 1.

We used an internationally accepted method, exposure-response function, to estimate all-cause deaths of residents due to air pollution [43]. The formula is as follows:

$$RR = e^{\beta(Ca-C0)} \quad (1)$$

$$E = B_0 \times E_{pop} \times (RR - 1)/RR \quad (2)$$

In this formula, E represents the number of residents mortality, B_0 represents the rate of the baseline mortality, E_{pop} represents the number of exposure residents, C_a and C_0 represent the concentration and threshold value of O_3, respectively. The World Health Organization (WHO) considered the threshold value of O_3 was 100 μg/m^3 in 2006. According to the latest research on the health effects of O_3 at low concentrations, 75.2 μg/m^3 was more suitable as the threshold value [44]. β is the concentration-response factor, which can be obtained through epidemiological

cohort studies [45]. In addition, we employed the value of statistical life methods to quantify the economic burden. For more information, please refer to our previous study [46].

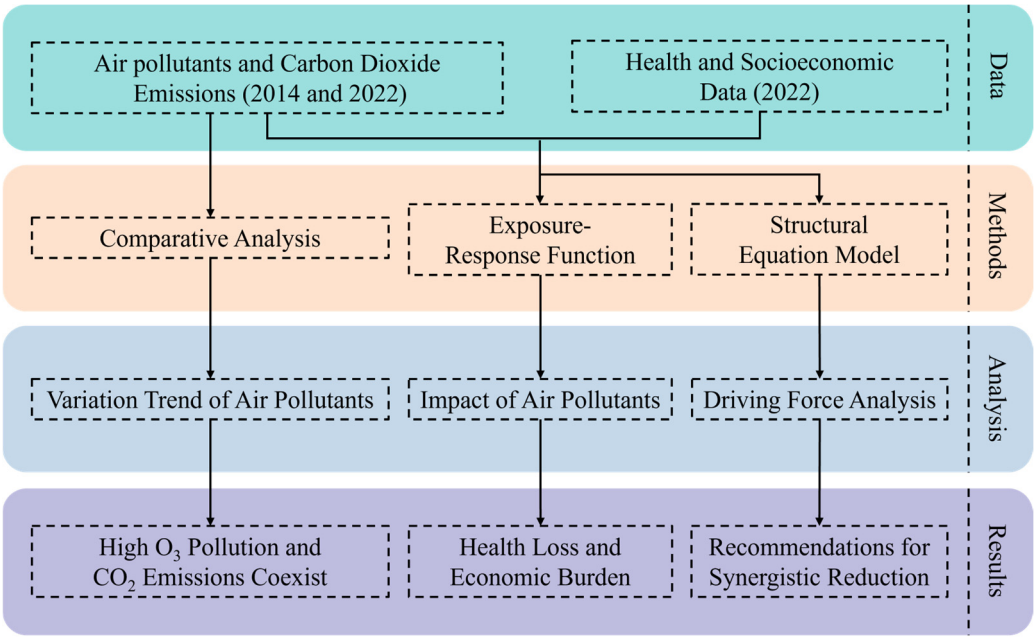

Figure 1. Schematic diagram of the study framework.

SEM is a key multivariate analysis tool that analyzes variable relationships through covariance matrices. In this model, observed variables represent directly measurable data collected during observation or experimentation. Latent variables capture abstract concepts, such as immeasurable causal factors, that are estimated through observed variables. In this study, we developed an SEM framework to examine linkages between socioeconomic data, CO_2 emissions, and O_3 pollution (Figure 2). We operatively implemented three latent variables: industrial scale, city size, and resident's activities. These were indirectly measured using fourteen observed socioeconomic variables (Table 1). In the initial model, residents' activities directly influenced pollutants (CO_2 emissions and O_3 pollution), while city size exerted indirect effects. Also, industrial scale not only directly influences pollutants but also indirectly affects them by impacting city size and residents' activities. Model reliability was assessed using the Akaike Information Criterion (AIC) and Comparative Fit Index (CFI), with pathways refined iteratively during model selection. The optimal model required that both the lowest AIC value and the CFI value be greater than 0.90. All SEM analyses were conducted in R 3.4.2 (Vienna, Austria) [47].

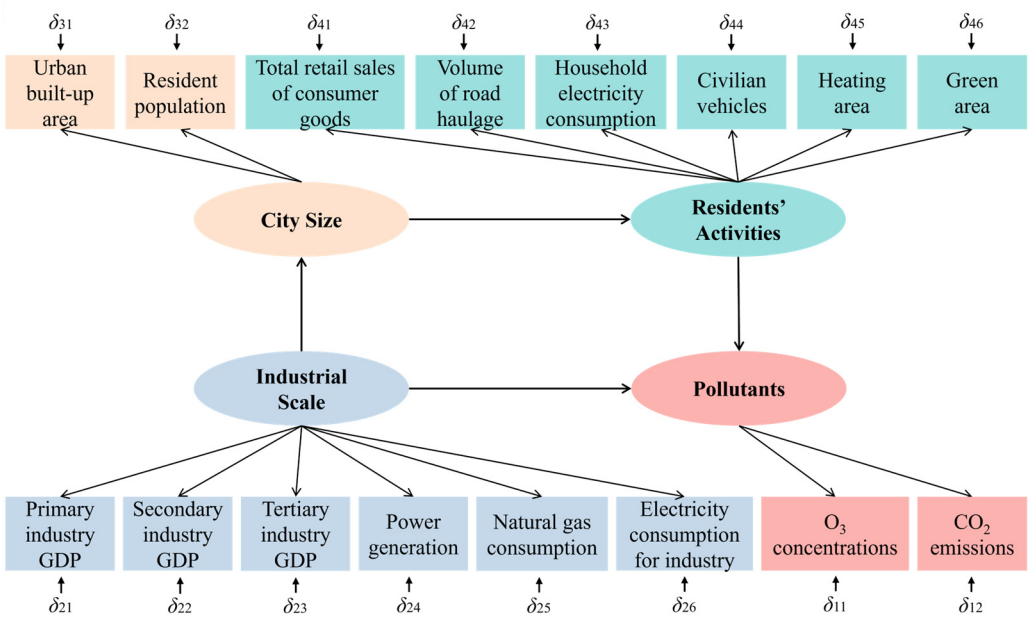

Figure 2. The initial frame for structural equation model. δ are measurement errors.

3. Results and Discussion

3.1. Temporal Variation of Air Pollution and CO_2 Emissions

In 2022, 238 Chinese cities up to national air quality standards, with annual mean $PM_{2.5}$ concentrations below 35 μg/m^3 (Figure 3A). Compared to 2014, $PM_{2.5}$ levels decreased across all Chinese cities in 2022 (Figure 3B). Especially in the Beijing-Tianjin-Hebei urban agglomeration, one of China's most important regions, seeing reductions of approximately 40 μg/m^3. These improvements demonstrate the exceptional effectiveness of China's urban air pollution controls following the 2013 Clean Air Act. However, despite the implementation of various emission reduction measures in urban areas, effective control of ground-level O_3 pollution remains inadequate. Most cities recorded higher O_3 concentrations in 2022 compared to 2014 (Figure 3D). The majority of polluted cities were concentrated on urban agglomeration, particularly the Central Plains and Yangtze River Delta agglomerations (Figure 3C). Consistent with O_3 pollution, urban CO_2 emissions also show rapid growth (Figure 3F). Higher-emitting cities are predominantly located in the Beijing-Tianjin-Hebei urban agglomeration, Central Plains urban agglomeration, and Yangtze River Delta urban agglomerations (Figure 3E). In conclusion, Chinese cities present a phenomenon where high O_3 pollution and high CO_2 emissions coexist, underscore the need for targeted control measures.

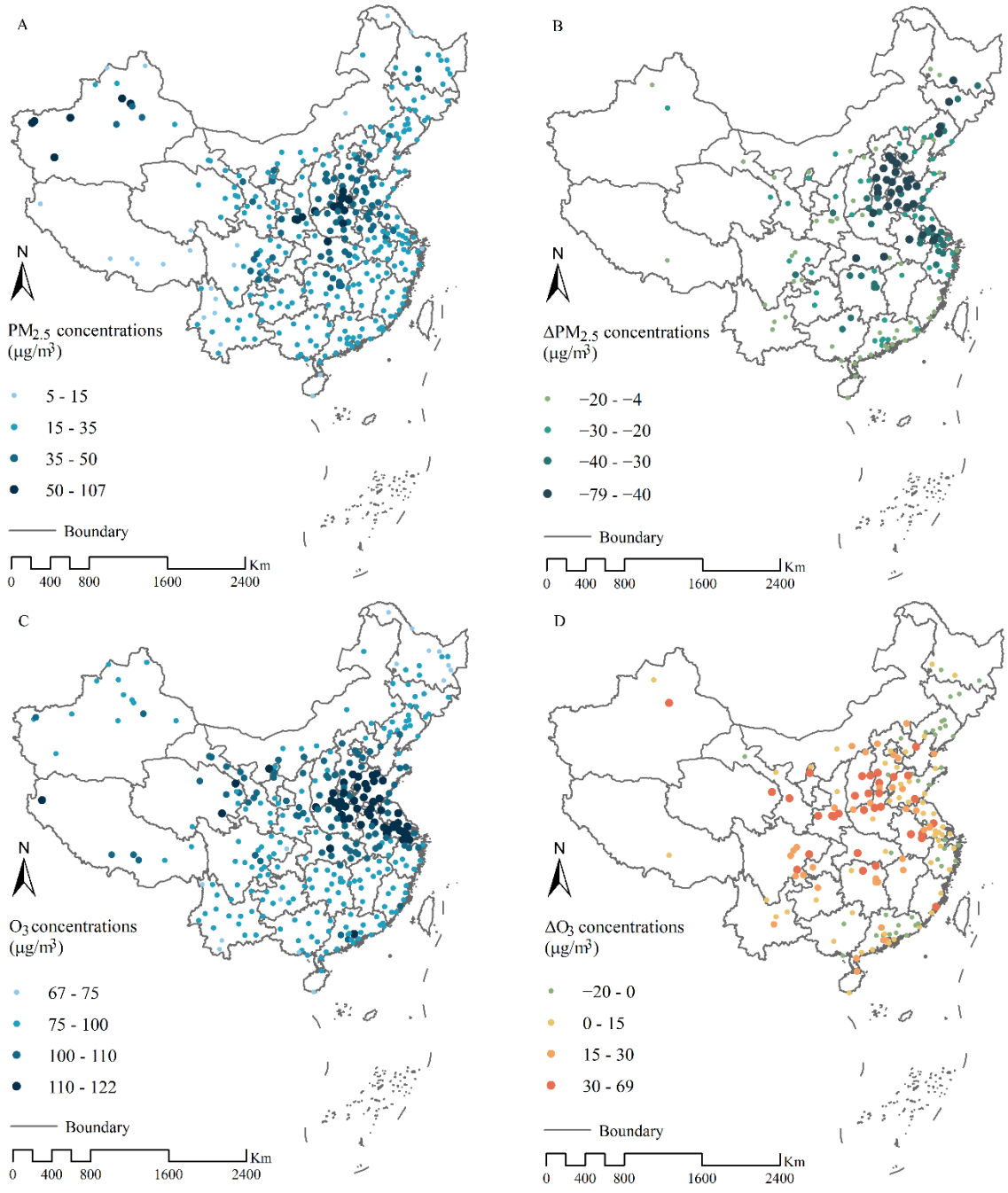

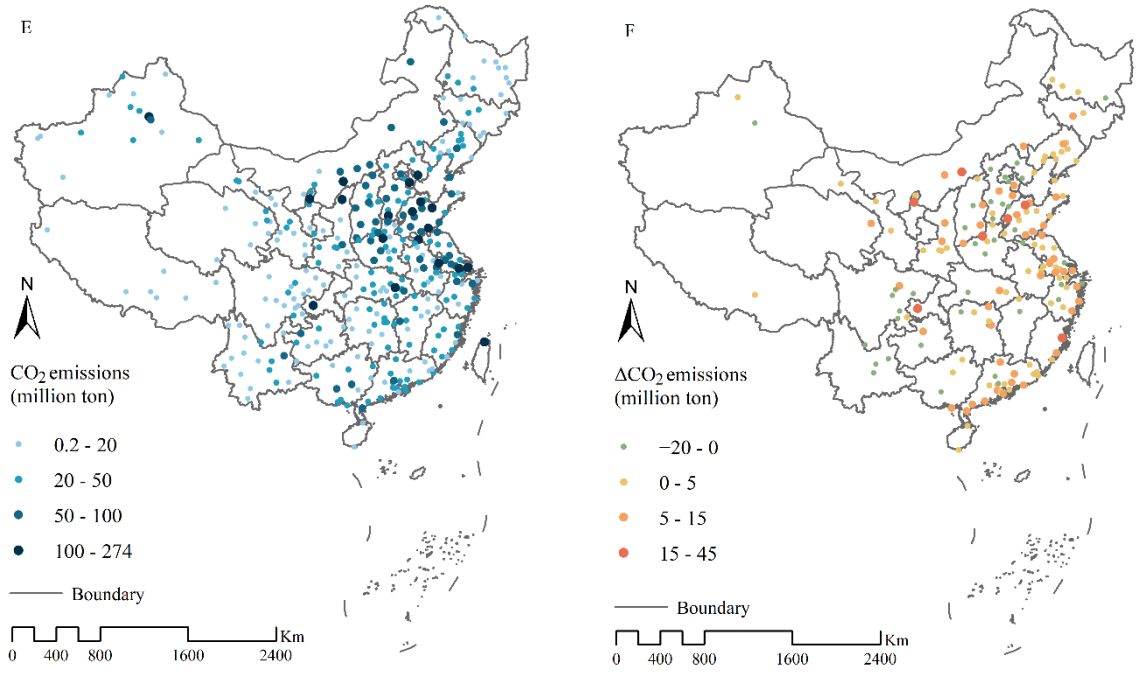

Figure 3. Interannual variations of urban air pollution and carbon dioxide emissions in China. (**A**,**C**,**E**) represent $PM_{2.5}$ concentrations, O_3 concentrations, and CO_2 emissions in different cities in 2022, respectively. (**B**,**D**,**F**) represent the interannual variations of $PM_{2.5}$ concentrations, O_3 concentrations, and CO_2 emissions in different cities from 2014 to 2022, respectively.

Meteorological parameters, such as sunshine duration, are critical drivers of O_3 formation, yet they are inherently uncontrollable through human intervention [48]. Adverse meteorological conditions may mask the potential benefits of emission reductions [49]. During the peak O_3 pollution period (April to September), continuous precipitation in southern China reduces sunshine duration and increases air humidity. These conditions suppress the photochemical conversion of precursors into O_3. Consequently, O_3 pollution levels are substantially higher in northern Chinese cities compared to southern cities, as illustrated by the national distribution pattern (Figure 3C). The timing and duration of O_3 pollution also vary significantly across major urban agglomerations due to distinct climatic regimes. Regions such as the Yangtze River Delta and the Central Plains urban agglomerations typically experience sufficient sunshine earlier, leading to an earlier onset and longer duration of elevated O_3 pollution. Conversely, the rainy seasons characteristic of the Pearl River Delta and Chengdu-Chongqing urban agglomerations delay the onset of significant O_3 pollution episodes.

While meteorological parameters are uncontrollable, reducing anthropogenic precursors (primarily NO_X and VOCs) is an effective strategy for mitigating O_3 pollution [11]. Existing research indicates that VOCs, including carbonyl compounds and monoterpenes, play critical roles in O_3 formation in China and other regions with high NO_X levels [50,51]. Positive matrix factorization analysis identified mobile and industrial emissions dominate in urban areas, whereas combustion-related emissions are more significant in rural areas [25,26].

Non-methane volatile organic compounds (NMVOCs) are the main indicators of urban VOCs emissions, and the establishment of corresponding emission inventories is the basis for controlling their total emissions. Chinese scholars have established detailed NMVOCs emission inventories based on the Multi-resolution Emission Inventory for China (http://meicmodel.org.cn/). The inventories mainly include the emission data of NMVOCs in the power, industrial, civil and transportation sectors.

Biogenic volatile organic compounds (BVOCs) from plants also contribute substantially to urban VOCs. Although green spaces are generally considered beneficial for urban air quality, their capacity to remove NO_2 and anthropogenic VOCs may be limited in northern cities [52]. BVOCs act as both precursors to O_3 and consumers of O_3 through oxidation reactions [21]. However, plant emissions of BVOCs in response to O_3 exposure remain poorly understood. Selecting appropriate plant species is therefore crucial for improving air quality while minimizing the harmful effects of BVOCs on human health [53].

Evidence also shows that O_3 in urban areas (e.g., Singapore, Jakarta, Kuala Lumpur, Bangkok, and Ho Chi Minh City) is sensitive to both NOx and VOC emissions, making synergistic control of both pollutants essential [54]. We suggest the regulatory policies should highlight the synergistic control of key precursors including NO_X and

VOCs to counteract the photochemical production of O_3 [55]. Reducing VOCs and NOx at a ratio of 0.5–1.2 could effectively curb O_3 increases [56].

3.2. Assessment of Health Loss and Economic Burden

Using the exposure-response function, we calculated the all-cause mortality attributable to O_3 pollution. The results indicate that approximately 198 × 10^3 all-cause deaths were linked to O_3 pollution in 2022 (Figure 4). Shanghai recorded the highest death toll (5548), followed by Wuhan (3920), Chengdu (3826), and Jinan (3546). The annual average O_3 concentration in 12 cities remained below the health impact threshold, resulting in zero O_3-related all-cause deaths. Based on O_3-related all-cause mortality, the estimated economic burden in China for 2022 reached US$15.48 billion, accounting for 0.09% of that year's GDP. Shanghai incurred the highest losses (US$1.21 billion), followed by Beijing (US$0.59 billion), Tianjin (US$0.39 billion), Jinan (US$0.31 billion), Linyi (US$0.27 billion), and Suzhou (US$0.27 billion). Collectively, these six cities accounted for 20% of the total economic burden.

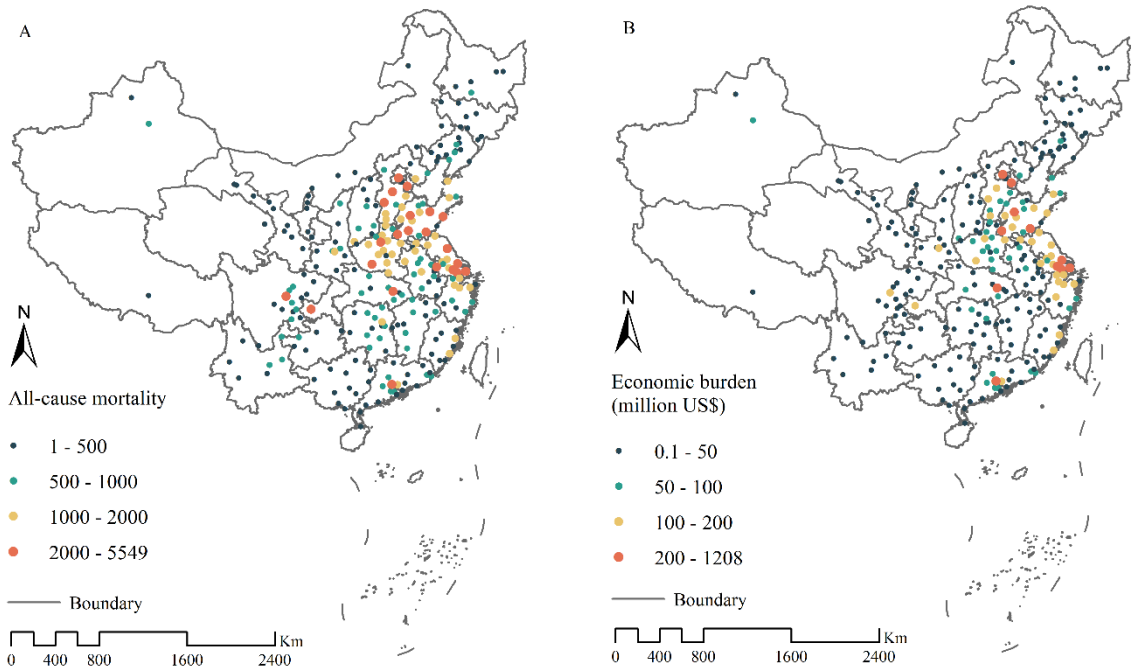

Figure 4. The distribution of all-cause mortality (**A**) and economic burden (**B**) related to ozone pollution.

Researchers find that the health and economic impacts of O_3 pollution are significantly lower than $PM_{2.5}$ [57]. However, O_3 is a kind of gas, and it is difficult for residents to have effective protection methods [58]. Notably, existing global assessments may understate O_3-related health impacts. Mid-latitude Asia (e.g., Shanghai and Wuhan) and the western United States exhibit high mortality burdens, contributing significantly to global O_3-attributable deaths [59]. Furthermore, substantial CO_2 emissions driving global climate change increase health risks. Extreme conditions like heatwaves are projected to exacerbate O_3 pollution threats to human health [21].

3.3. The Results of SEM

We used AIC and CFI indices to determine the stability of the model. The optimal model achieved the lowest AIC value, and the CFI reached 0.91 after removing the interference parameter (natural gas consumption) (Table 2).

The optimal SEM results are presented in Figure 5. Among the latent variables, both industrial scale and resident's activities showed a stronger influence on pollutants (total influence = 0.45) than city size (total influence = 0.1). For observed variables, tertiary industry GDP (total influence = 0.12) and secondary industry GDP (total influence = 0.11) had the highest impact on pollutants, while heating area (total influence = 0.03) had the lowest.

Table 2. Analysis of model stability.

Remove	AIC	CFI	Remove	AIC	CFI
Natural gas consumption	1227	0.91	Total retail sales of consumer goods	1395	0.84
Primary industry GDP	1277	0.9	Household electricity consumption	1403	0.83
Tertiary industry GDP	1285	0.87	Volume of road haulage	1415	0.83
Secondary industry GDP	1323	0.87	Heating area	1440	0.82
Electricity consumption for industry	1367	0.85	Power generation	1487	0.81
Green area	1372	0.84	Civilian vehicles	1510	0.79

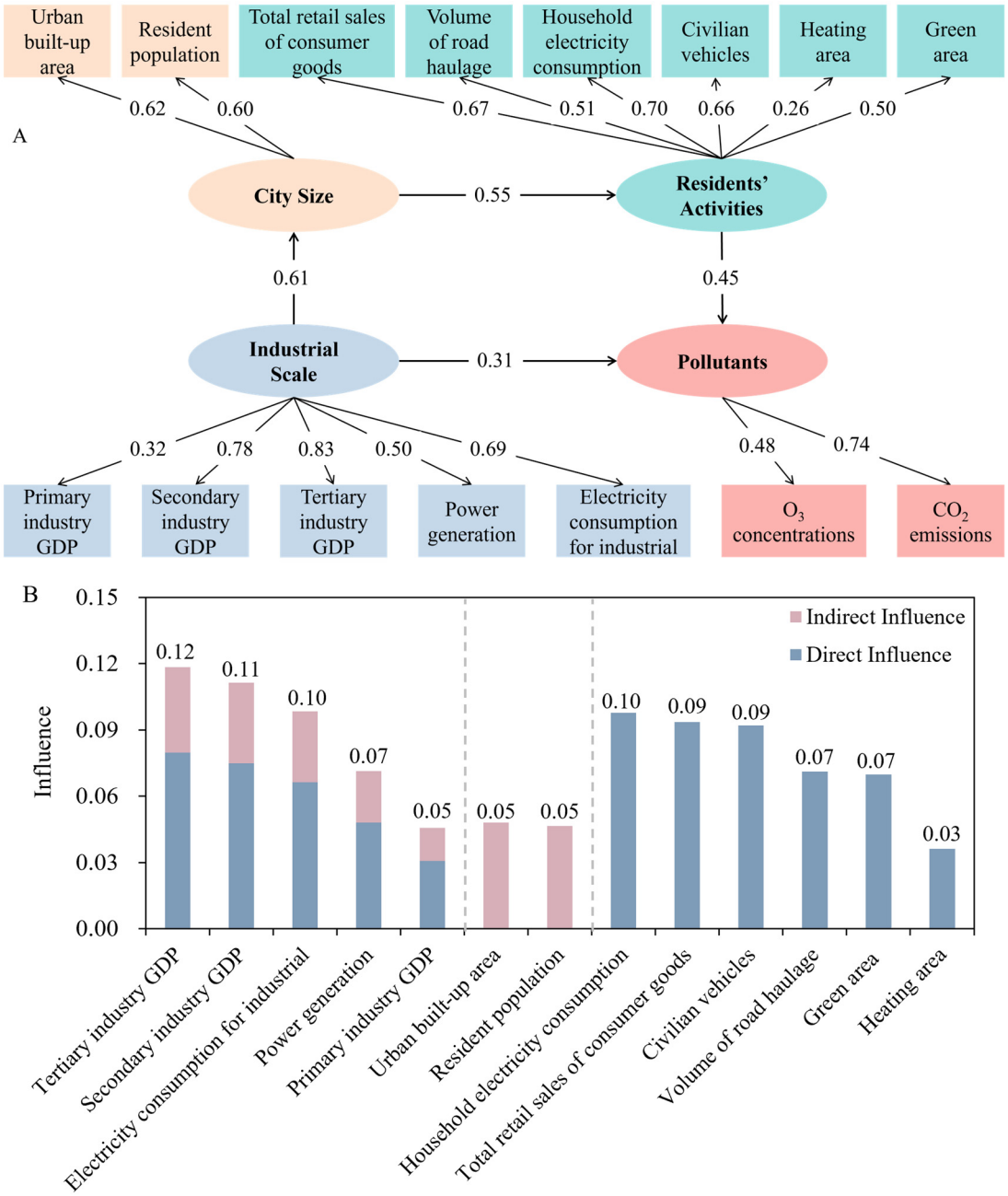

Figure 5. Results of optimal model and contributions of multiple driving forces on O_3 pollution and CO_2 emissions. The numbers in (**A**) represent path coefficients. (**B**) shows the standardized values of multiple driving forces.

Industrial scale emerges as the primary contributor to both O_3 pollution and CO_2 emissions in China (Figure 5). Tertiary and secondary industry GDP represent the largest socioeconomic drivers, which indicate the urgency of industrial optimization in China. Fossil fuel use and material consumption (e.g., solvents) during production and transportation, which release substantial CO_2 and O_3 precursors [28,60]. Globally, fossil fuel combustion accounts for over 75% of greenhouse gas emissions and nearly 90% of total CO_2 emissions [1]. The construction sector is

a major consumer of non-renewable energy and a significant source of greenhouse gases, necessitating a transition to net-zero carbon emissions by 2050. Construction activities currently represent 36% of global energy consumption and 39% of global CO_2 emissions [30]. Similarly, the steel industry, cement industry and urea industry are the key emitters of CO_2 and air pollutants [33,34,61]. However, these contributions will be reduced because of international cooperation and technological advances. In China, thermal power generation dominates electricity production and constitutes the highest proportion of industrial CO_2 emissions. Consequently, accurate carbon accounting for this sector is critical for national emissions inventories [29]. Electricity-related carbon emissions include both direct emissions from power generation and indirect emissions from consumption. Driven by environmental imperatives, thermal power is gradually being replaced by clean energy.

City size exerts a significant indirect influence on pollutants. Large populations and extensive urban built-up areas, key characteristics of city size, typically contribute to increased precursor and CO_2 emissions [2,27]. Our findings indicate that resident population and urban built-up areas exert comparable indirect effects on pollutants. In China, urbanization rate and resident population are the principal drivers of carbon emissions and air pollution [2].

As economies develop, residents increasingly use natural gas, electricity, and vehicles, further affecting air quality [42]. Cities, as primary hubs of economic activity and endpoints for goods/services consumption, account for most global greenhouse gas and pollutant emissions. Rising global temperatures and growing health awareness have substantially increased air conditioning usage. Vapor compression systems, significant CO_2 emitters, also impact stratospheric O_3 depletion through refrigerant leakage. Similarly, cooking with electricity or natural gas generates substantial precursors and CO_2 [37]. Recent studies show that food consumption represents the largest carbon footprint component in household behaviors across 11 major Japanese metropolitan areas [62]. Vehicle exhaust remains another major emission source in cities [42]. Modeling indicates that widespread zero-emission vehicle adoption in Los Angeles could simultaneously reduce summer NO_X emissions by 28% and CO_2 emissions by 41%, resulting in moderate, non-linear O_3 mitigation benefits [28]. Consumer goods contribute to precursors throughout their lifecycle, including production and consumption stages [63]. Precursors and CO_2 emissions from the transportation and consumption stages are mainly local [37].

It is important to note that while industrial GDP demonstrated the strongest impact on O_3 pollution and CO_2 emissions in China, this does not imply industrial scale is the primary source in every prefecture-level city. All thirteen observed variables in our analysis contribute to pollutants either directly or indirectly. Rather than emphasizing the relative contribution of specific drivers in our SEM results, our intent is for policymakers to holistically evaluate all factors when designing legislation and strategies to fundamentally curb rising urban O_3 pollution and CO_2 emissions. Accordingly, we propose comprehensive control measures in the following discussion.

3.4. Policy Recommendations

To achieve sustainable development, the Chinese government issued “Air Pollution Prevention Action Plan” in 2013, “Peak Carbon Dioxide Emissions and Carbon Neutrality” in 2020, and “Synergistic Pollution Reduction and Carbon Mitigation Implementation Plan” in 2022. These mitigation efforts are expected to concurrently reduce co-emitted air pollutants and carbon.

To mitigate climate change and achieve net-zero emissions, CO_2 removal (CDR) pathways for capturing, storing, and conversion CO_2 are rapidly developing. Direct air capture technologies include physical absorption (via ionic liquids), chemical looping, and cryogenic separation [31]. Crucially, low-cost sorbents regenerable at low temperatures could overcome current technological limitations [64]. Gigatonne-scale geological storage represents a cornerstone of carbon sequestration. However, effective implementation requires deeper understanding of subsurface storage mechanisms and trapping dynamics. Further research is essential to optimize these techniques and elucidate their fundamental processes [1]. Overcoming deployment barriers through enhanced financial incentives and public acceptance programs will enable climate-relevant CO_2 storage volumes [65]. CO_2 conversion serves as a complementary strategy to geological storage [1]. Emerging approaches include chemical methods (plasma catalysis, electrochemical, photochemical) and biological pathways (photosynthetic and non-photosynthetic) [31]. Electrochemical conversion shows particular promise for sustainable production of value-added chemicals [66,67], utilizing proton-exchange membrane systems, nanocrystalline cubic molybdenum carbide, and single-atom-based electrocatalysts to efficiently convert CO_2 into formic acid, carbon monoxide, and ethanol respectively [68–70].

While CDR is essential for carbon neutrality, with projections indicating multi-gigatonne annual removal by 2050, current technologies remain economically unviable [71,72]. Moreover, excessive reliance on future CDR carries significant risks, including delayed emissions reductions, fossil infrastructure lock-in, and sustainability threats from resource competition. Consequently, governments must maintain focus on proven non-CDR strategies

(e.g., continuous emissions reduction, renewable energy deployment, and electrification), rather than banking on uncertain future CDR scaling [73].

Based on our findings, we propose five targeted policy recommendations for coordinated control of CO_2 emissions and O_3 pollution: (1) Adopt clean energy and low-pollution solvents. Traditional construction materials like cement release significant CO_2 during production, while solvents generate substantial O_3 precursors [33]. Geopolymer-based 3D printing offers a renewable, low-carbon alternative [74]; (2) Reduce transportation emissions. The fossil fuel-dependent transportation sector, particularly petroleum-based systems, poses major challenges for reducing CO_2 and precursor emissions [32]. China's forthcoming stringent National VII standards aim to achieve co-reduction of carbon and pollutants; (3) Mitigate residential consumption impacts. Daily use of volatile chemical products (printing inks, adhesives, personal care items) contributes significantly [75]. Current linear plastic production and consumption generate unsustainable waste, pollution, and CO_2 emissions, undermining climate goals [76]. We recommend public environmental health education and corporate development of alternatives; (4) Optimize urban greening. We can use plants to absorb CO_2 in the atmosphere and reduce O_3 pollution in urban areas [77]. However, the latest research reminds us that we should pay attention to the biogenic emissions [78]. For example, forestation is widely proposed for CO_2 removal, but forestation increased aerosol scattering, methane and O_3 following increased biogenic organic emissions [79]. Additionally, forestation decreased surface albedo, which yielded a positive radiative forcing; and (5) Enhance regional coordination. Strengthen joint control on regional sources of urban agglomeration, implement coordinated reductions of precursor emissions, and establish O_3 pollution early-warning system to issue O_3 dynamics [37,80].

4. Conclusions

We analyzed China's current air pollution status, finding it characterized by high levels of O_3 pollution and CO_2 emissions. All-cause mortality related to O_3 pollution reached nearly 0.2 million deaths in 2022. Subsequently, we employed an SEM to analyze the synergistic control mechanisms for these two gases. The results indicated that the tertiary industry GDP and secondary industry GDP contribute more significantly than the other twelve socioeconomic parameters examined. The quantified formation mechanisms of O_3 pollution and CO_2 emissions can provide more integrated information for the reduction policy. Our research confirms the effectiveness of SEM in quantifying these mechanisms. In the future, we could incorporate more sector-specific information into the analysis.

Author Contributions

Conceptualization: X.H. Data curation: X.H. and J.L. Methodology: X.H. and S.Z. (Shuang Zhao). Funding acquisition: S.L. Investigation: X.H. and S.L. Software: S.Z. (Shuang Zhao) and S.Z. (Siyang Zhou). Visualization: S.Z. (Shuang Zhao) and T.Y. Writing—original draft: X.H. Writing—review & editing: X.H. and S.L. All authors have read and agreed to the published version of the manuscript.

Funding

The work was supported by the National Natural Sciences Fund Project (No. 42271097, 42307129) and the National Key Research and Development Project (No. 2022YFF1303204).

Institutional Review Board Statement

Not applicable.

Informed Consent Statement

Not applicable.

Data Availability Statement

The air pollution data is available through the link https://www.cnemc.cn/ [Dataset] (accessed on 1 April 2025). The total carbon dioxide emission data is available at https://edgar.jrc.ec.europa.eu/emissions_data_and_maps [Dataset] (accessed on 10 April 2025). Residents' health data is available at https://www.stats.gov.cn/sj/ndsj/ (accessed on 20 April 2025) and https://www.ncmi.cn/ [Dataset] (accessed on 20 April 2025). Socioeconomic data is available at https://www.stats.gov.cn/sj/ndsj/ [Dataset] (accessed on 30 April 2025). R software is available at https://www.r-project.org/ [Software] (accessed on 1 June 2025).

Acknowledgments

We thank the teachers and students who provide help for the data processing of this paper. I would also like to thank the National Natural Science Foundation of China, the Ministry of Science and Technology of the People's Republic of China and the National Social Science Foundation of China for its funding.

Conflicts of Interest

The authors declare no conflicts of interest. Given the role as Editor-in-Chief, Shiliang Liu had no involvement in the peer review of this paper and had no access to information regarding its peer review process. Full responsibility for the editorial process of this paper was delegated to another editor of the journal.

Use of AI and AI-Assisted Technologies

No AI tools were utilized for this paper.

References

1. Bashir, A.; Ali, M.; Patil, S.; et al. Comprehensive review of CO_2 geological storage: Exploring principles, mechanisms, and prospects. *Earth-Sci. Rev.* **2024**, *249*, 104672. https://doi.org/10.1016/j.earscirev.2023.104672.
2. Li, X.J.; Lin, C.X.; Lin, M.C.; Drivers and spatial patterns of carbon emissions from residential buildings: An empirical analysis of Fuzhou city (China). *Build. Environ.* **2024**, *257*, 111534. https://doi.org/10.1016/j.buildenv.2024.111534.
3. Huang, X.P.; Zheng, W.; Li, Y.C.; et al. Ozone formation in a representative urban environment: Model discrepancies and critical roles of oxygenated volatile organic compounds. *Environ. Sci. Technol. Lett.* **2025**, *12*, 297–304. https://doi.org/10.1021/acs.estlett.4c01026.
4. Zhang, J.F.; Wei, Y.J.; Fang, Z.F. Ozone pollution: A major health hazard worldwide. *Front. Immunol.* **2019**, *10*, 2518. https://doi.org/10.3389/fimmu.2019.02518.
5. Wang, T.; Chen, X.; Yao, Y.; et al. Pro-thrombotic changes in response to ambient ozone exposure exacerbated by temperatures. *Environ. Sci. Technol.* **2025**, *59*, 8391–8401. https://doi.org/10.1021/acs.est.4c13457.
6. Feng, Z.Z.; Uddling, J.; Tang, H.Y.; et al. Comparison of crop yield sensitivity to ozone between open-top chamber and free-air experiments. *Global Chang. Biol.* **2018**, *24*, 2231–2238. https://doi.org/10.1111/gcb.14077.
7. Mills, G.; Sharps, K.; Simpson, D.; et al. Ozone pollution will compromise efforts to increase global wheat production. *Global Chang. Biol.* **2018**, *24*, 3560–3574. https://doi.org/10.1111/gcb.14157.
8. Xie, B.; Zhao, Z.P.; Xu, L.; et al. Nitrogen deposition mitigates ozone-induced stress in Quercus aliena: Transcriptomic and metabolomic perspectives. *Environ. Pollut.* **2025**, *373*, 126158. https://doi.org/10.1016/j.envpol.2025.126158.
9. Lu, X.F.; Li, J.; Zhou, X.Y.; et al. Negative effects of elevated ozone levels on soil microbial characteristics: A meta-analysis. *Plant Soil* **2025**, *513*, 2177–2192. https://doi.org/10.1007/s11104-025-07309-6.
10. Jiao, G.; Chen, L.; Li, K.; et al. Worsened ozone pollution exacerbates the loss of agricultural production in China. *J. Geophys. Res. Atmos.* **2025**, *130*, e2024JD042781. https://doi.org/10.1029/2024JD042781.
11. Yang, J.Z.; Zhao, Y.; Cao, J.; et al. Co-benefits of carbon and pollution control policies on air quality and health till 2030 in China. *Environ. Int.* **2021**, *152*, 106482. https://doi.org/10.1016/j.envint.2021.106482.
12. Yang, X.Y.; Wu, K.; Wang, H.L.; et al. Summertime ozone pollution in Sichuan Basin, China: Meteorological conditions, sources and process analysis. *Atmos. Environ.* **2020**, *226*, 117392. https://doi.org/10.1016/j.atmosenv.2020.117392.
13. Wang, L.L.; Yang, X.C.; Dong, J.W.; et al. Evolution of surface ozone pollution pattern in eastern China and its relationship with different intensity heatwaves. *Environ. Pollut.* **2023**, *338*, 122725. https://doi.org/10.1016/j.envpol.2023.122725.
14. Lin, M.Y.; Xie, Y.Y.; De Smedt, I.; et al. Ozone pollution extremes in southeast China exacerbated by reduced uptake by vegetation during hot droughts. *Geophys. Res. Lett.* **2025**, *52*, e2025GL114934. https://doi.org/10.1029/2025GL114934.
15. Ding, S.; Wei, Z.W.; Liu, S.L.; et al. Uncovering the evolution of ozone pollution in China: A spatiotemporal characteristics reconstruction from 1980 to 2021. *Atmos. Res.* **2024**, *307*, 107472. https://doi.org/10.1016/j.atmosres.2024.107472.
16. Zhu, X.C.; Dong, H.X.; Huang, Y.W.; et al. Assessing ozone pollution and climate change impacts on winter wheat: Flux modeling vs. dose-response modeling. *J. Environ. Manag.* **2025**, *387*, 125767. https://doi.org/10.1016/j.jenvman.2025.125767.
17. Nowroz, F.; Hasanuzzaman, M.; Siddika, A.; et al. Elevated tropospheric ozone and crop production: Potential negative effects and plant defense mechanisms. *Front. Plant Sci.* **2024**, *14*, 1244515. https://doi.org/10.3389/fpls.2023.1244515.
18. Lei, Y.D.; Yue, X.; Liao, H.; et al. Global perspective of drought impacts on ozone pollution episodes. *Environ. Sci. Technol.* **2022**, *56*, 3932–3940. https://doi.org/10.1021/acs.est.1c07260.
19. Liu, C.Q.; Shi, K. A review on methodology in O_3-NOx-VOC sensitivity study. *Environ. Pollut.* **2021**, *291*, 118249. https://doi.org/10.1016/j.envpol.2021.118249.
20. Zohdirad, H.; Namin, M.M.; Ashrafi, K.; et al. Temporal variations, regional contribution, and cluster analyses of ozone

and NOx in a middle eastern megacity during summertime over 2017–2019. *Environ. Sci. Pollut. Res.* **2021**, *29*, 16233–16249. https://doi.org/10.1007/s11356-021-14923-1.

21. Gao, C.; Zhang, X.L.; Lun, X.X.; et al. BVOCs' role in dynamic shifts of summer ozone formation regimes across China and policy implications. *J. Environ. Manag.* **2025**, *376*, 124150. https://doi.org/10.1016/j.jenvman.2025.124150.
22. Zhao, Y.F.; Gao, J.; Cai, J.Y.; et al. Real-time tracing VOCs, O_3 and $PM_{2.5}$ emission sources with vehicle-mounted proton transfer reaction mass spectrometry combined differential absorption lidar. *Atmos. Pollut. Res.* **2021**, *12*, 146–153. https://doi.org/10.1016/j.apr.2021.01.008.
23. Zhang, Y.L.; Yang, X.X.; Lin, X.; et al. Characteristics of ozone pollution and VOCs source analysis in the northern cities of Zhejiang, China. *Atmos. Pollut. Res.* **2025**, *16*, 102429. https://doi.org/10.1016/j.apr.2025.102429.
24. Guo, J.; Zhang, X.S.; Gao, Y.; et al. Evolution of ozone pollution in China: What track will it follow? *Environ. Sci. Technol.* **2023**, *57*, 109–117. https://doi.org/10.1021/acs.est.2c08205.
25. Liu, Z.Q.; Xu, W.L.; Zhu, S.N.; et al. Elucidating ozone formation mechanisms in the central Yangtze River Delta region, China: Urban and rural differences. *Environ. Pollut.* **2025**, *372*, 125979. https://doi.org/10.1016/j.envpol.2025.125979.
26. Qiu, Y.Q.; Li, X.; Chai, W.X.; et al. Insights into ozone pollution control in urban areas by decoupling meteorological factors based on machine learning. *Atmos. Chem. Phys.* **2025**, *25*, 1749–1763. https://doi.org/10.5194/acp-25-1749-2025.
27. Yang, G.F.; Liu, Y.H.; Li, W.L.; et al. Association analysis between socioeconomic factors and urban ozone pollution in China. Environ. *Sci. Pollut. R.* **2023**, *30*, 17597–17611. https://doi.org/10.1007/s11356-022-23298-w.
28. Zhu, Q.D.; Schwantes, R.H.; Stockwell, C.E.; et al. Incorporating cooking emissions to better simulate the impact of zero-emission vehicle adoption on ozone pollution in Los Angeles. *Environ. Sci. Technol.* **2025**, *59* 5672–5682. https://doi.org/10.1021/acs.est.5c00902.
29. Li, Y.W.; Yang, X.X.; Du, E.S.; et al. A review on carbon emission accounting approaches for the electricity power industry. *Appl. Energy* **2024**, *359*, 122681. https://doi.org/10.1016/j.apenergy.2024.122681.
30. Chen, L.; Huang, L.P.; Hua, J.M.; et al. Green construction for low-carbon cities: A review. *Environ. Chem. Lett.* **2023**, *21*, 1627–1657. https://doi.org/10.1007/s10311-022-01544-4.
31. Mohammed, S.; Eljack, F.; Al-Sobhi, S.; et al. A systematic review: The role of emerging carbon capture and conversion technologies for energy transition to clean hydrogen. *J. Clean. Prod.* **2024**, *447*, 141506. https://doi.org/10.1016/j.jclepro.2024.141506.
32. Zhang, Q.; Gu, B.H.; Zhang, H.Y.; et al. Emission reduction mode of China's provincial transportation sector: Based on "Energy+" carbon efficiency evaluation. *Energy Policy* **2023**, *177*, 113556. https://doi.org/10.1016/j.enpol.2023.113556.
33. Liu, X.; Yang, L.; Du, J.H.; et al. Carbon and air pollutant emissions forecast of China's cement industry from 2021 to 2035. *Resour. Conserv. Recycl.* **2024**, *204*, 107498. https://doi.org/10.1016/j.resconrec.2024.107498.
34. Song, X.C.; Du, S.; Deng, C.N.; et al. Carbon emissions in China's steel industry from a life cycle perspective: Carbon footprint insights. *J. Environ. Sci.* **2025**, *148*, 650–664. https://doi.org/10.1016/j.jes.2023.04.027.
35. He, D.C.; Li, F.H.; Wu, M.; et al. Emission of volatile organic compounds (VOCs) from application of commercial pesticides in China. *J. Environ. Manag.* **2022**, *314*, 115069. https://doi.org/10.1016/j.jenvman.2022.115069.
36. Zhang, Y.P.; Guo, X.H.; Zhu, X.D. Strong diurnal variability of carbon dioxide flux over algae-shellfish aquaculture ponds revealed by eddy covariance measurements. *Agric. Ecosyst. Environ.* **2023**, *348*, 108426. https://doi.org/10.1016/j.agee.2023.108426.
37. He, S.Q.; Yang, Y.; Wang, H.L.; et al. Source attribution of near-surface ozone pollution in Jiangsu Province of China over 2013–2019. *Atmos. Environ.* **2025**, *352*, 121205. https://doi.org/10.1016/j.atmosenv.2025.121205.
38. Xia, X.S.; Ren, P.Y.; Wang, X.H.; et al. The carbon budget of China: 1980–2021. *Sci. Bull.* **2024**, *69*, 114–124. https://doi.org/10.1016/j.scib.2023.11.016.
39. Zhao, S.; Liu, S.L.; Hou, X.Y.; et al. Temporal dynamics of SO_2 and NO_X pollution and contributions of driving forces in urban areas in China. *Environ. Pollut.* **2018**, *242*, 239–248. https://doi.org/10.1016/j.envpol.2018.06.085.
40. Wang, J.F.; Qiu, Y.; He, S.T.; et al. Investigating the driving forces of NO_X generation from energy consumption in China. *J. Clean. Prod.* **2018**, *184*, 836–846. https://doi.org/10.1016/j.jclepro.2018.02.305.
41. He, C.; Hong, S.; Zhang, L.; Global, continental, and national variation in $PM_{2.5}$, O_3, and NO_2 concentrations during the early 2020 COVID-19 lockdown. *Atmos. Pollut. Res.* **2021**, *12*, 136–145. https://doi.org/10.1016/j.apr.2021.02.002.
42. Al-Hemoud, A.; Gasana, J.; Alajeel, A.; et al. Ambient exposure of O_3 and NO_2 and associated health risk in Kuwait. *Environ. Sci. Pollut. Res.* **2021**, *28*, 14917–14926. https://doi.org/10.1007/s11356-020-11481-w.
43. Pope, C.A.; Turner, M.C.; Burnett, R.T.; et al. Relationships between fine particulate air pollution, cardiometabolic disorders, and cardiovascular mortality. *Circ. Res.* **2015**, *116*, 108–115. https://doi.org/10.1161/circresaha.116.305060.
44. Lelieveld, J.; Evans, J.S.; Fnais, M.; et al. The contribution of outdoor air pollution sources to premature mortality on a global scale. *Nature* **2015**, *525*, 367–371. https://doi.org/10.1038/nature15371.
45. Turner, M.C.; Jerrett, M.; Pope, C.A., III; et al. Long-term ozone exposure and mortality in a large prospective study. Am. J. *Resp. Crit. Care.* **2016**, *193*, 1134–1142. https://doi.org/10.1164/rccm.201508-1633OC.

46. Hou, X.Y.; Guo, Q.H.; Hong, Y.; et al. Assessment of $PM_{2.5}$-related health effects: A comparative study using multiple methods and multi-source data in China. *Environ. Pollut.* **2022**, *306*, 119381. https://doi.org/10.1016/j.envpol.2022.119381.
47. R Development Core Team. *R: A Language and Environment for Statistical Computing*; R Foundation for Statistical Computing: Vienna, Austria, 2017; ISBN 3-900051-07-0. Available online: http://www.R-project.org/ (accessed on 1 June 2025).
48. Zhang, X.; Lu, X.; Wang, F.; et al. Enhanced late spring ozone in Southern China by early onset of the South China Sea summer monsoon. *J. Geophys. Res. Atmos.* **2024**, *129*, e2023JD039029. https://doi.org/10.1029/2023JD039029.
49. Lu, S.; Gong, S.; Chen, J.; et al. Composite effects of ENSO and EASM on summer ozone pollution in two regions of China. *J. Geophys. Res. Atmos.* **2022**, *127*, e2022JD036938. https://doi.org/10.1029/2022JD036938.
50. Bao, J.M.; Zhang, X.; Wu, Z.H.; et al. Atmospheric carbonyl compounds are crucial in regional ozone heavy pollution: Insights from the Chengdu Plain Urban Agglomeration, China. *Atmos. Chem. Phys.* **2025**, *25*, 1899–1916. https://doi.org/10.5194/acp-25-1899-2025.
51. Wang, H.C.; Ma, X.F.; Tan, Z.F.; et al. Anthropogenic monoterpenes aggravating ozone pollution. *Natl. Sci. Rev.* **2022**, *9*, nwac103. https://doi.org/10.1093/nsr/nwac103.
52. Setälä, H.; Viippola, V.; Rantalainen, A.L.; et al. Does urban vegetation mitigate air pollution in northern conditions? *Environ. Pollut.* **2013**, *183*, 104–112. https://doi.org/10.1016/j.envpol.2012.11.010.
53. Carriero, G.; Brunetti, C.; Fares, S.; et al. BVOC responses to realistic nitrogen fertilization and ozone exposure in silver birch. *Environ. Pollut.* **2016**, *213*, 988–995. https://doi.org/10.1016/j.envpol.2015.12.047.
54. Fang, T.T.; Hu, J.; Gu, Y.F.; et al. Response of ozone to current and future emission scenarios and the resultant human health impact in Southeast Asia. *Environ. Int.* **2025**, *197*, 109333. https://doi.org/10.1016/j.envint.2025.109333.
55. Li, X.B.; Yuan, B.; Parrish, D.D.; et al. Long-term trend of ozone in southern China reveals future mitigation strategy for air pollution. *Atmos. Environ.* **2022**, *269*, 118869. https://doi.org/10.1016/j.atmosenv.2021.118869.
56. Xing, J.; Ding, D.; Wang, S.X.; et al. Quantification of the enhanced effectiveness of NO_X control from simultaneous reductions of VOC and NH_3 for reducing air pollution in the Beijing-Tianjin-Hebei region, China. *Atmos. Chem. Phys.* **2018**, *18*, 7799–7814. https://doi.org/10.5194/acp-18-7799-2018.
57. Xie, Y.; Dai, H.C.; Zhang, Y.X.; et al. Comparison of health and economic impacts of $PM_{2.5}$ and ozone pollution in China. *Environ. Int.* **2019**, *130*, 104881. https://doi.org/10.1016/j.envint.2019.05.075.
58. Qi, C.; Shang, L.; Yang, W.; et al. Maternal exposure to O_3 and NO_2 may increase the risk of newborn congenital hypothyroidism: A national data-based analysis in China. *Environ. Sci. Pollut. Res.* **2021**, *28*, 34621–34629. https://doi.org/10.1007/s11356-021-13083-6.
59. Wang, Y.; Yang, Y.J.; Yuan, Q.Q.; et al. Substantially underestimated global health risks of current ozone pollution. *Nat. Commun.* **2025**, *16*, 102. https://doi.org/10.1038/s41467-024-55450-0.
60. Dantas, G.; Siciliano, B.; da Silva, C.M.; et al. A reactivity analysis of volatile organic compounds in a Rio de Janeiro urban area impacted by vehicular and industrial emissions. *Atmos. Pollut. Res.* **2020**, *11*, 1018–1027. https://doi.org/10.1016/j.apr.2020.02.017.
61. Hu, Q.; Zhou, W.L.; Qi, S.; et al. Pulsed co-electrolysis of carbon dioxide and nitrate for sustainable urea synthesis. *Nat. Sustain.* **2024**, *7*, 442–451. https://doi.org/10.1038/s41893-024-01302-0.
62. Huang, L.Q.; Long, Y.; Chen, J.D.; et al. Sustainable lifestyle: Urban household carbon footprint accounting and policy implications for lifestyle-based decarbonization. *Energy Policy* **2023**, *181*, 113696. https://doi.org/10.1016/j.enpol.2023.113696.
63. Shin, H.M.; Mckone, T.E.; Bennett, D.H. Contribution of low vapor pressure-volatile organic compounds (LVP-VOCs) from consumer products to ozone formation in urban atmospheres. *Atmos. Environ.* **2015**, *108*, 98–106. https://doi.org/10.1016/j.atmosenv.2015.02.067.
64. Li, H.G.; Zick, M.E.; Trisukhon, T.; et al. Capturing carbon dioxide from air with charged-sorbents. *Nature* **2024**, *630*, 654–659. https://doi.org/10.1038/s41586-024-07449-2.
65. Krevor, S.; de Coninck, H.; Gasda, S.E.; et al. Subsurface carbon dioxide and hydrogen storage for a sustainable energy future. *Nat. Rev. Earth Environ.* **2023**, *4*, 102–118. https://doi.org/10.1038/s43017-022-00376-8.
66. Abdellah, A.M.; Ismail, F. Impact of palladium/palladium hydride conversion on electrochemical CO_2 reduction via in-situ transmission electron microscopy and diffraction. *Nat. Commun.* **2024**, *15*, 938. https://doi.org/10.1038/s41467-024-45096-3.
67. Jiang, M.H.; Wang, H.Z.; Zhu, M.F.; et al. Review on strategies for improving the added value and expanding the scope of CO_2 electroreduction products. *Chem. Soc. Rev.* **2024**, *53*, 5149–5189. https://doi.org/10.1039/d3cs00857f.
68. Fang, W.S.; Guo, W.; Lu, R.H.; et al. Durable CO_2 conversion in the proton-exchange membrane system. *Nature* **2024**, *626*, 86–91. https://doi.org/10.1038/s41586-023-06917-5.
69. Khoshooei, M.A.; Wang, X.J.; Vitale, G.; et al. An active, stable cubic molybdenum carbide catalyst for the high-temperature reverse water-gas shift reaction. *Science* **2024**, *384*, 540–546. https://doi.org/10.1126/science.adl1260.
70. Singh, A.; Barman, S.; Rahimi, F.A.; et al. Atomically dispersed Co^{2+} in a redox-active COF for electrochemical CO_2

reduction to ethanol: Unravelling mechanistic insight through operando studies. *Energy Environ. Sci.* **2024**, *17*, 2315–2325. https://doi.org/10.1039/d3ee02946h.

71. Baskaran, D.; Saravanan, P.; Nagarajan, L.; et al. An overview of technologies for capturing, storing, and utilizing carbon dioxide: Technology readiness, large-scale demonstration, and cost. *Chem. Eng. J.* **2024**, *491*, 151998. https://doi.org/10.1016/j.cej.2024.151998.
72. Fuhrman, J.; Bergero, C.; Weber, M.; et al. Diverse carbon dioxide removal approaches could reduce impacts on the energy-water-land system. *Nat. Clim. Chang.* **2023**, *13*, 341–350. https://doi.org/10.1038/s41558-023-01604-9.
73. Ampah, J.D.; Jin, C.; Liu, H.F.; et al. Prioritizing non-carbon dioxide removal mitigation strategies could reduce the negative impacts associated with large-scale reliance on negative emissions. *Environ. Sci. Technol.* **2024**, *58*, 3755–3765. https://doi.org/10.1021/acs.est.3c06866.
74. Chen, K.L.; Liu, Q.; Chen, B.; et al. Effect of raw materials on the performance of 3D printing geopolymer: A review. *J. Build. Eng.* **2024**, *84*, 108501. https://doi.org/10.1016/j.jobe.2024.108501.
75. Mcdonald, B.C.; De Gouw, J.A.; Gilman, J.B.; et al. Volatile chemical products emerging as largest petrochemical source of urban organic emissions. *Science* **2018**, *359*, 760–764. https://doi.org/10.1126/science.aaq0524.
76. Vidal, F.; van der Marel, E.R.; Kerr, R.W.F.; et al. Designing a circular carbon and plastics economy for a sustainable future. *Nature* **2024**, *626*, 45–57. https://doi.org/10.1038/s41586-023-06939-z.
77. Araminienė, V.; Sicard, P.; Anav, A.; et al. Trends and inter-relationships of ground-level ozone metrics and forest health in Lithuania. *Sci. Total. Environ.* **2019**, *658*, 1265–1277. https://doi.org/10.1016/j.scitotenv.2018.12.092.
78. Wang, W.P.; Wang, Y.; Chen, X.Y.; et al. The future underlying differential response of surface ozone to biogenic emissions in China (2019–2060). *Atmos. Environ.* **2025**, *352*, 121206. https://doi.org/10.1016/j.atmosenv.2025.121206.
79. Weber, J.; King, J.A.; Abraham, N.L.; et al. Chemistry-albedo feedbacks offset up to a third of forestation's CO_2 removal benefits. *Science* **2024**, *383*, 860–864. https://doi.org/10.1126/science.adg6196.
80. Guo, R.Y.; Shi, G.M.; Zhang, D.; et al. An observed nocturnal ozone transport event in the Sichuan Basin, Southwestern China. *J. Environ. Sci.* **2024**, *138*, 10–18. https://doi.org/10.1016/j.jes.2023.02.054.